

Tracking pereirine and flavopereirine in pau-pereira by using Raman and SERS spectroscopies

Lenize F. Maia^a, Marcia R. Almeida^b, Dhieniffer F. Carvalho^a, Nathália M. P. Rosa^c, Antonio Carlos Sant'Ana^a, Luiz Antonio S. Costa^c, Vanessa End de Oliveira^d, Angelo C. Pinto^{b†}, Luiz Fernando C. de Oliveira^a

^aNEEM/Departamento de Química, Universidade Federal de Juiz de Fora, Campus Universitario s/n, Martelos, Juiz de Fora, MG, 36033-620, Brazil.

^bFaculdade de Tecnologia - Universidade do Estado do Rio de Janeiro, Rodovia Presidente Dutra km 298, Polo Industrial, Rezende, RJ, 27537-000, Brazil.

^cNEQC/Departamento de Química, Universidade Federal de Juiz de Fora, Campus Universitario s/n, Martelos, Juiz de Fora, MG, 36033-620, Brazil.

^dDepartamento de Ciências da Natureza, Universidade Federal Fluminense, Campus Universitário de Rio das Ostras, Rua Recife, s/n, Jardim Bela Vista, Rio das Ostras, RJ, 28890-000, Brazil.

^eInstituto de Química - Universidade Federal do Rio de Janeiro Instituto de Química, Ilha do Fundão, 21945-970, Rio de Janeiro, RJ, Brazil ([†] *in memoriam*).

Figures

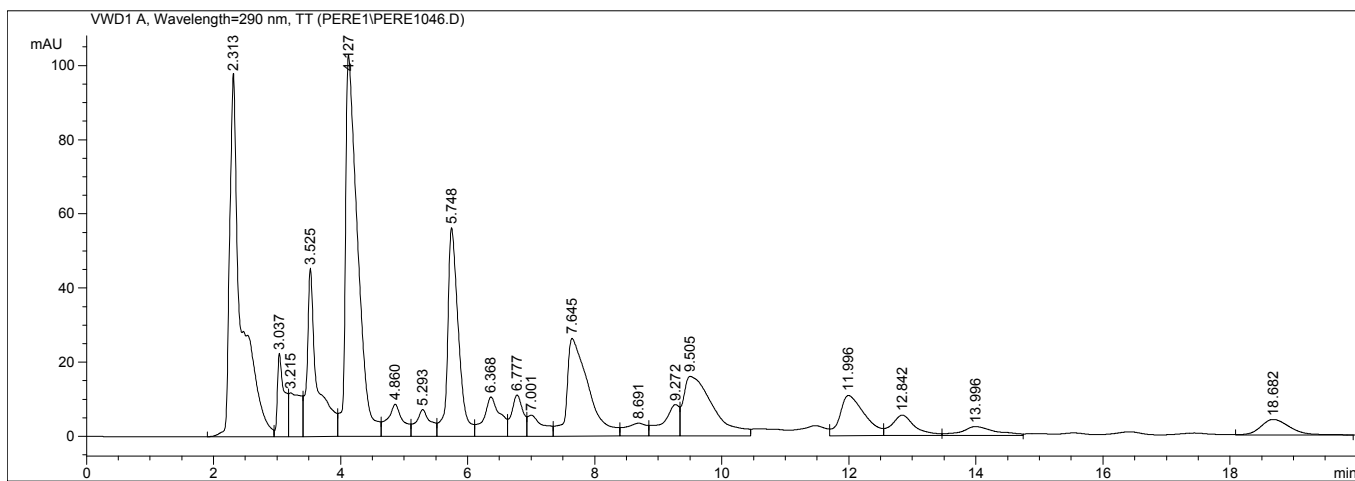


Figure S1. HPLC profile of pereirine (Agilent LC 1100 Chemstation A 10.02 - 2003). Column: DBC-18 ($5\mu\text{m}$, 250mm x 4,6mm), $\lambda=290\text{nm}$, ACN:H₂O 20:80 (v/v) + H₃PO₄ 0,1%, rate: 1mL/min, 10 μL).

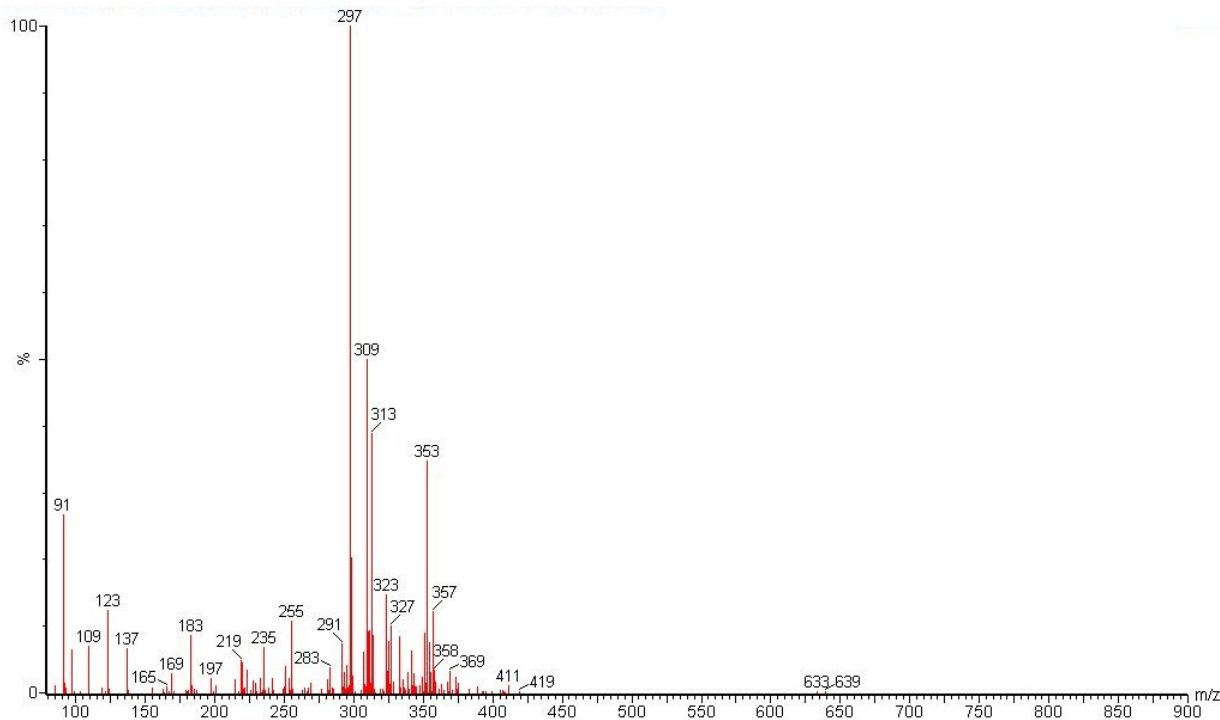


Figure S2. ESI-MS spectra of PR- velosimine: [M-H⁻ 291], geissoschizoline: [M-H⁻ 297], geissoschizidine: [M-H⁻ 351].

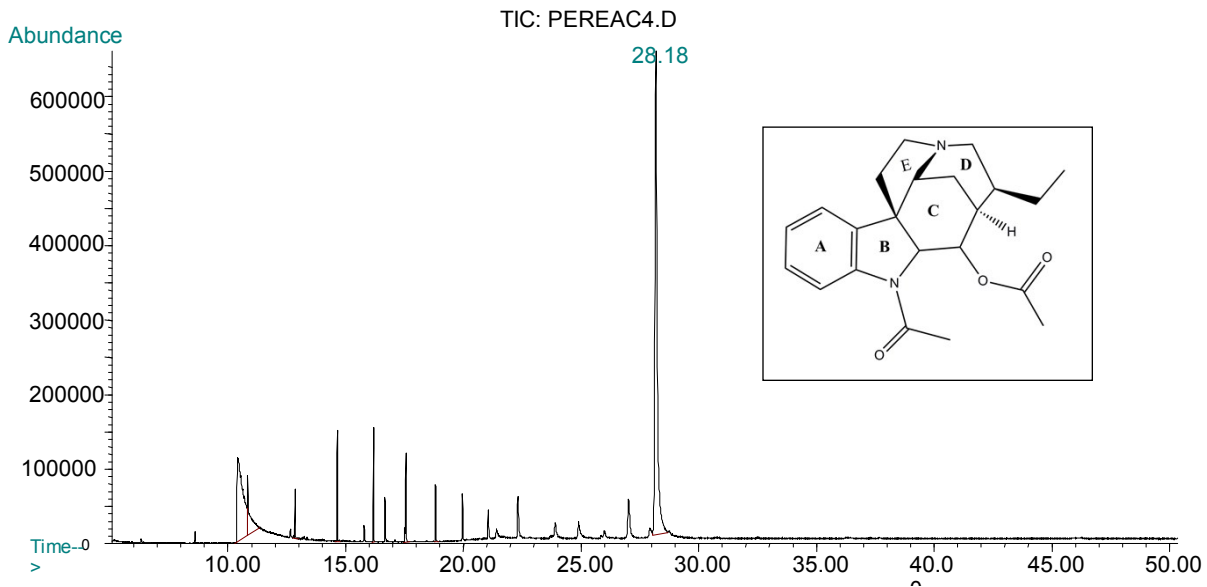


Figure S3. GC chromatogram obtained from diacetylgeissoschizoline. DB1 capillary column (30 m×0.25 mm), flow rate of carrier gas (Helium) at 1.0 mL/min, splitless.

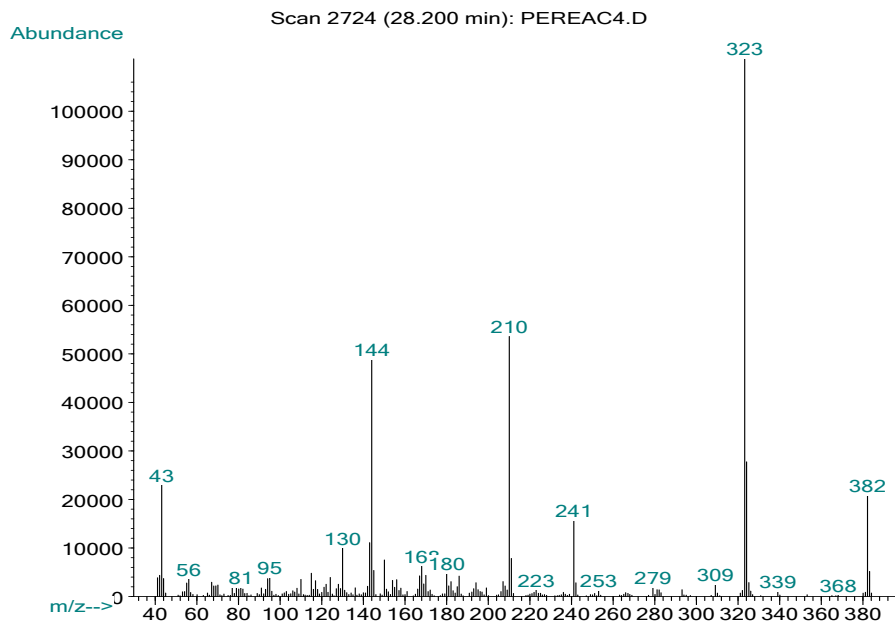


Figure S4. EI-MS spectrum of diacetylgeissoschizoline.

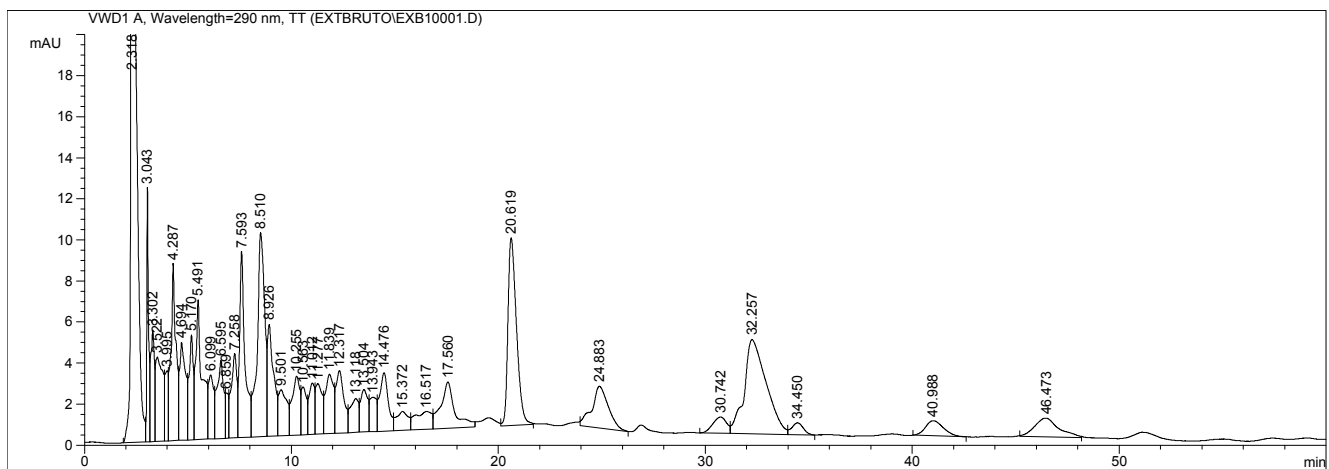


Figure S5. HPLC profile of the ethanolic crude extract of MAT06 sample (Agilent LC 1100 Chemstation A 10.02 - 2003). Column: DBC-18 (5 μ m, 250mm x 4,6mm), λ = 290nm, ACN:H₂O 20:80 (v/v) + H₃PO₄ 0,1%, rate: 1mL/min, 10 μ L).

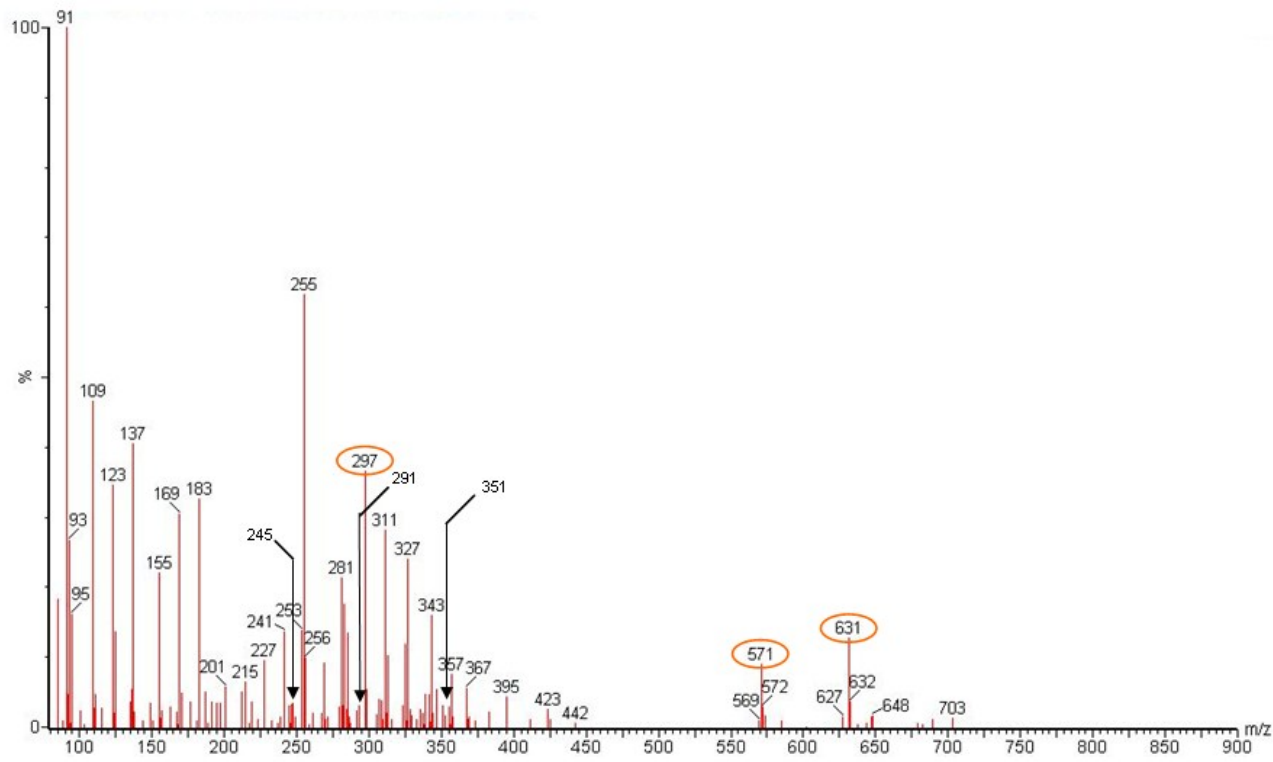


Figure S6. ESI-MS from the ethanolic crude extract of MAT06 sample. Spectrum was acquired using a Micromass Q-Tof mass spectrometer (Waters corporation MA), Software: Mass Lynx, versão 4.0 - 2004. ESI parameters were set as follow: capillary voltage, 1600V from negative mode; source temperature, 100°C; desolvation temperature, 120 °C; reference cone voltage: 20V. [M-H]⁻ 631: geissospermine; m/z 571: geissolosimine; m/z 351: geissosquizine; m/z 297: geissosquizoline; m/z 291: velosimine; m/z 245: flavopereirine.

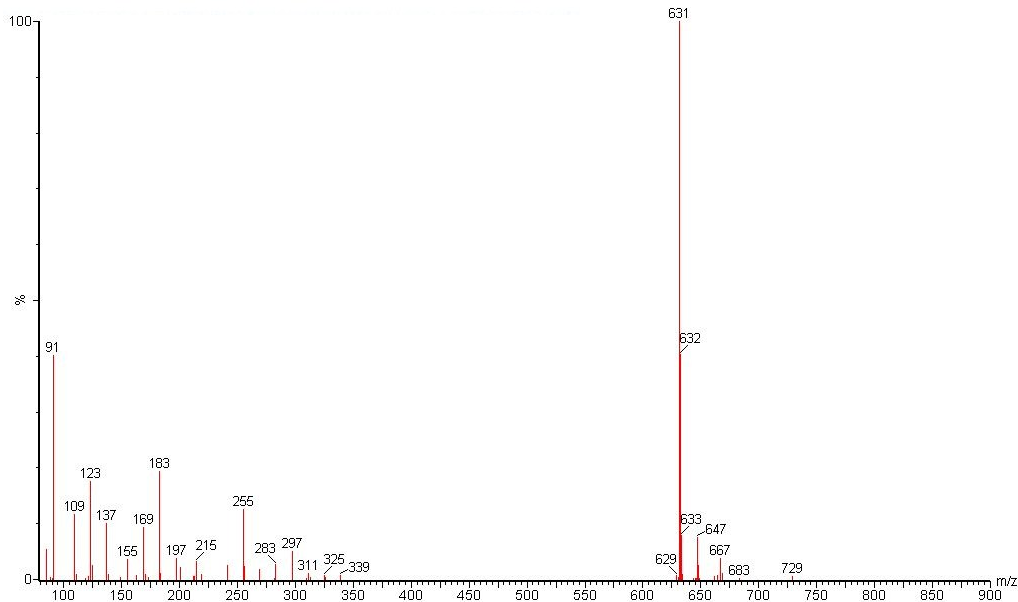


Figure S7. ESI-MS of geissospermine acquired using a Micromass Q-Tof mass spectrometer (Waters corporation MA), Software: Mass Lynx, versão 4.0 - 2004. ESI parameters were set as follow: capillary voltage, 1600V from negative mode; source temperature, 100°C; desolvation temperature, 120 °C; reference cone voltage: 20V.

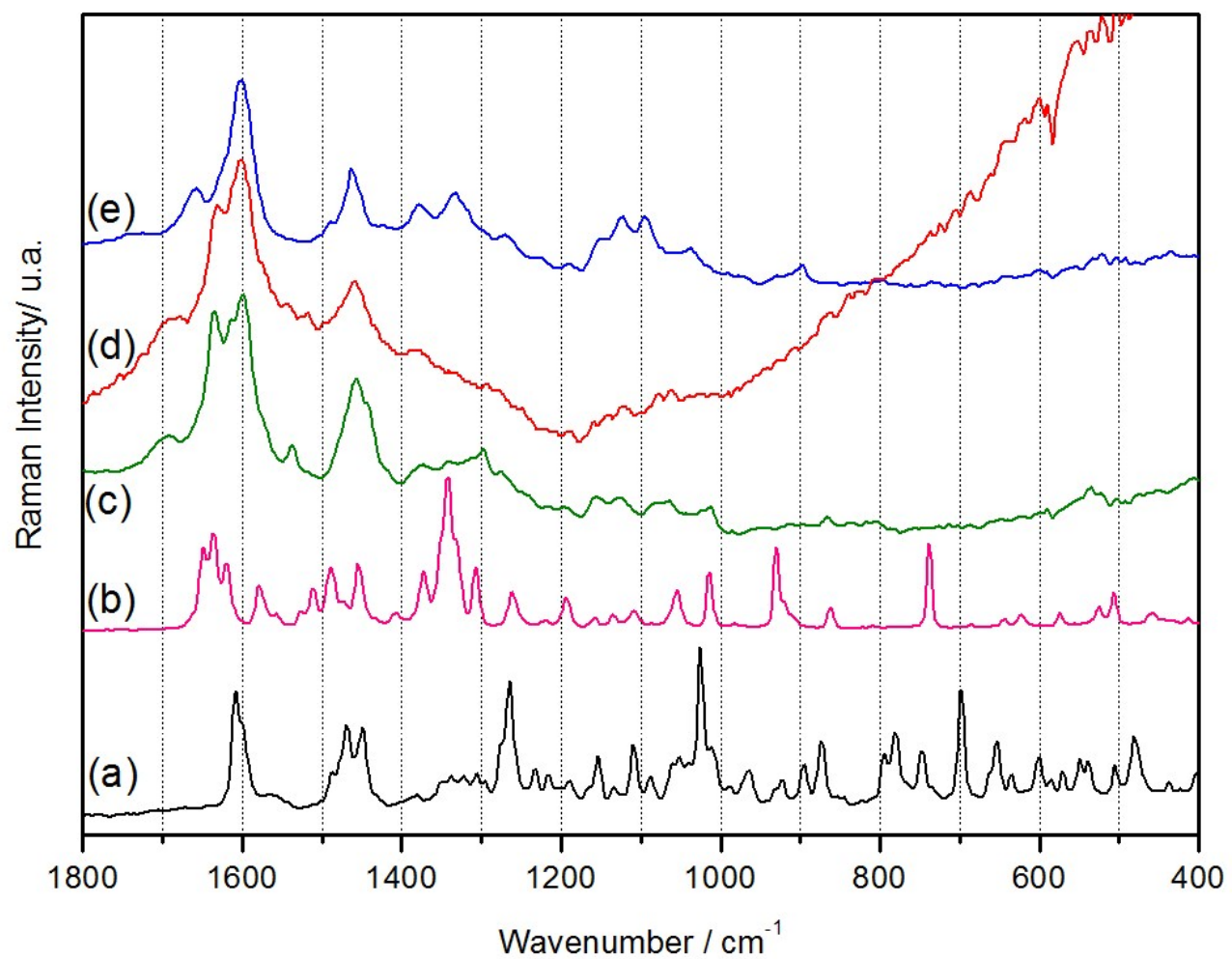


Figure S8. AC sample: (a) PR; (b) FP; (c) crude extract; (d) infusion and (e) bark.

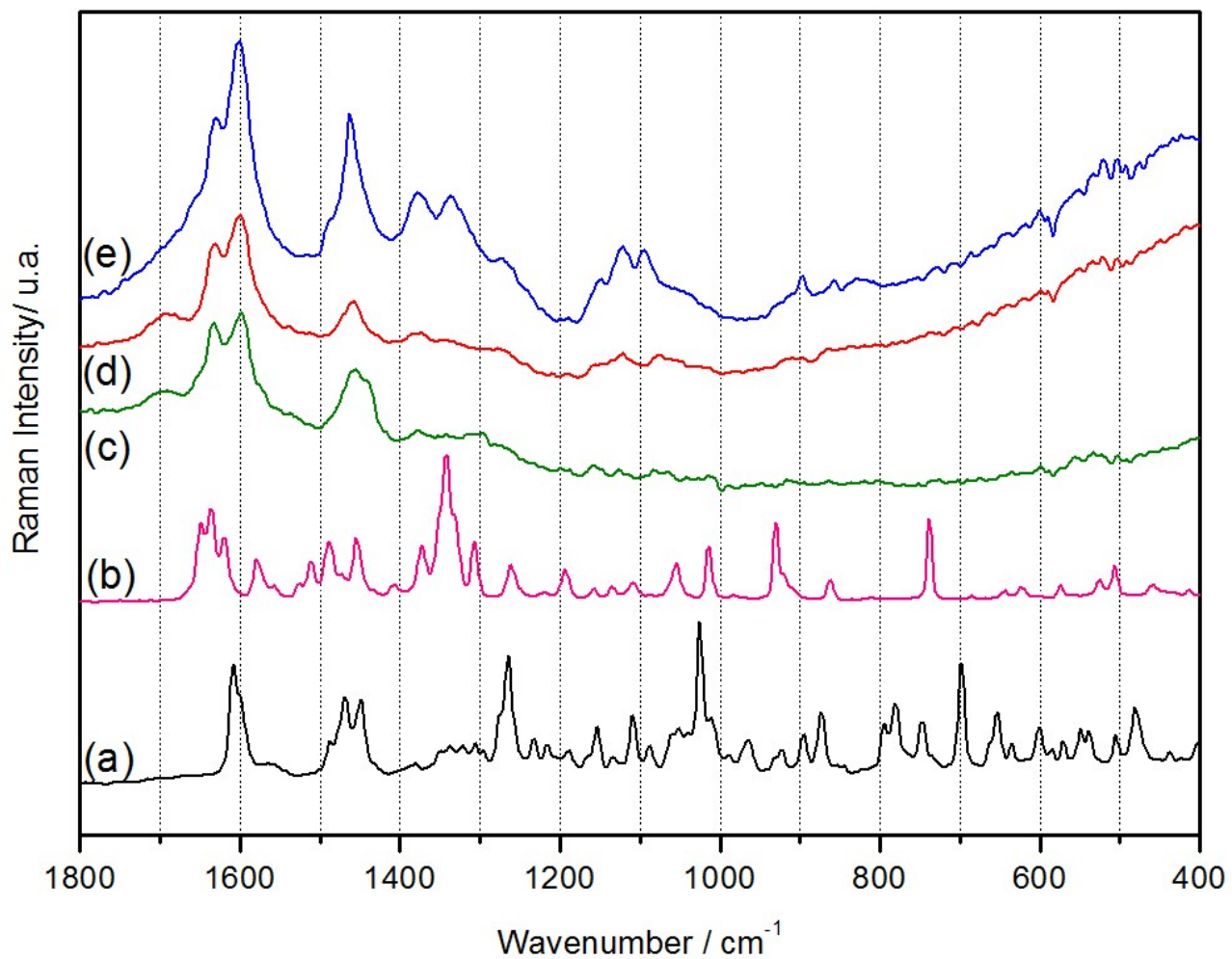


Figure S9. ACVL sample: (a) PR; (b) FP; (c) crude extract; (d) infusion and (e) bark.

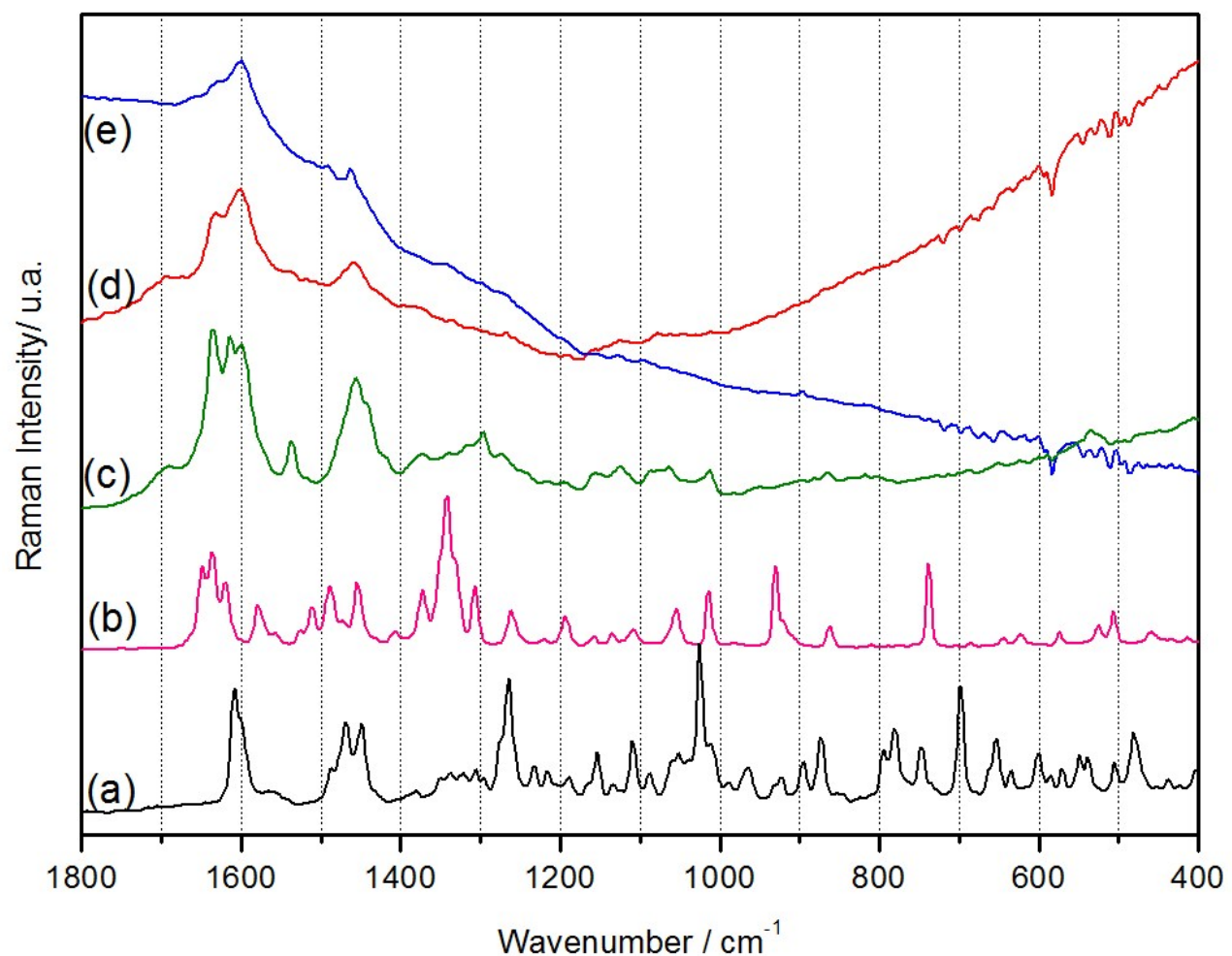


Figure S10. EN sample: (a) PR; (b) FP; (c) crude extract; (d) infusion and (e) bark.

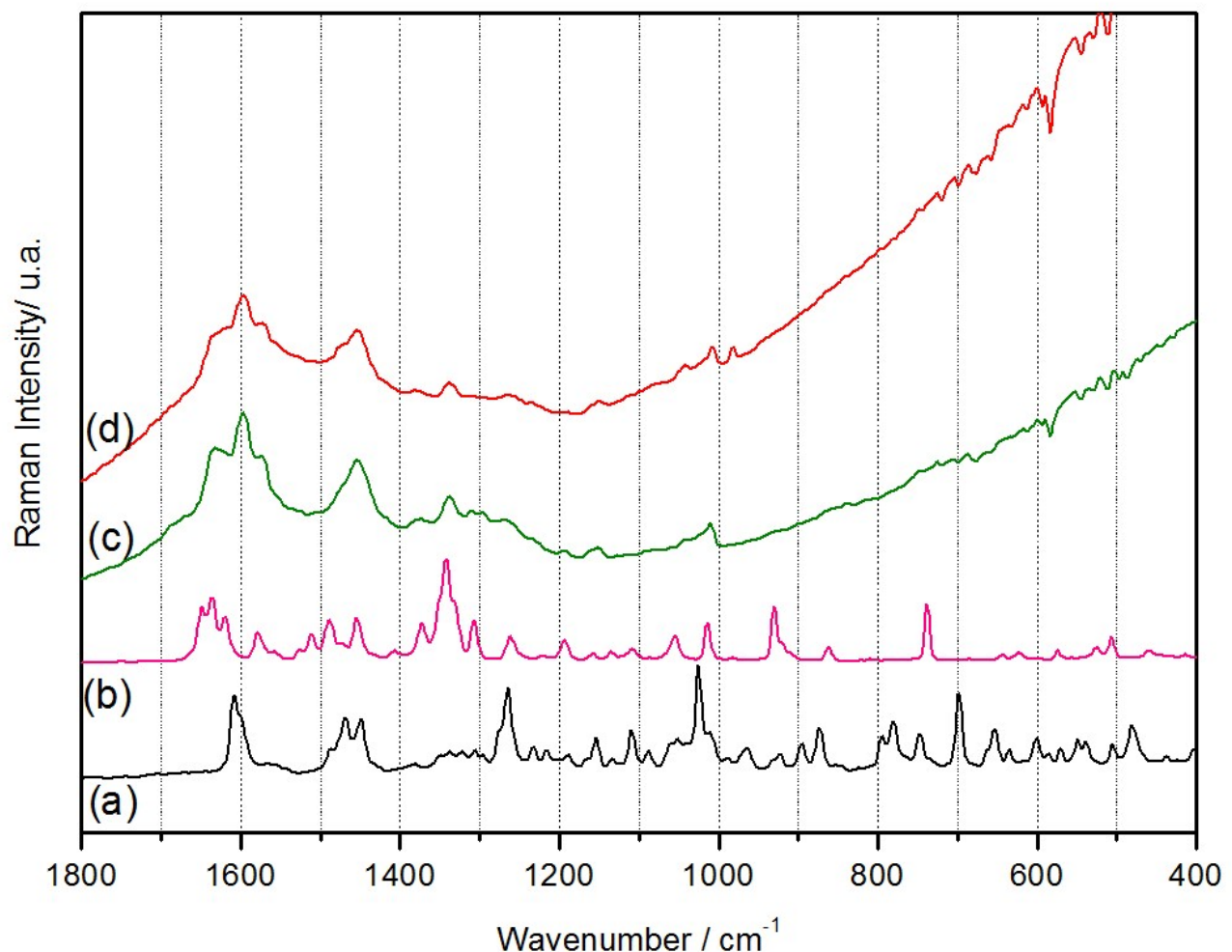


Figure S11. FJ sample: (a) PR; (b) FP; (c) crude extract and (d) infusion.

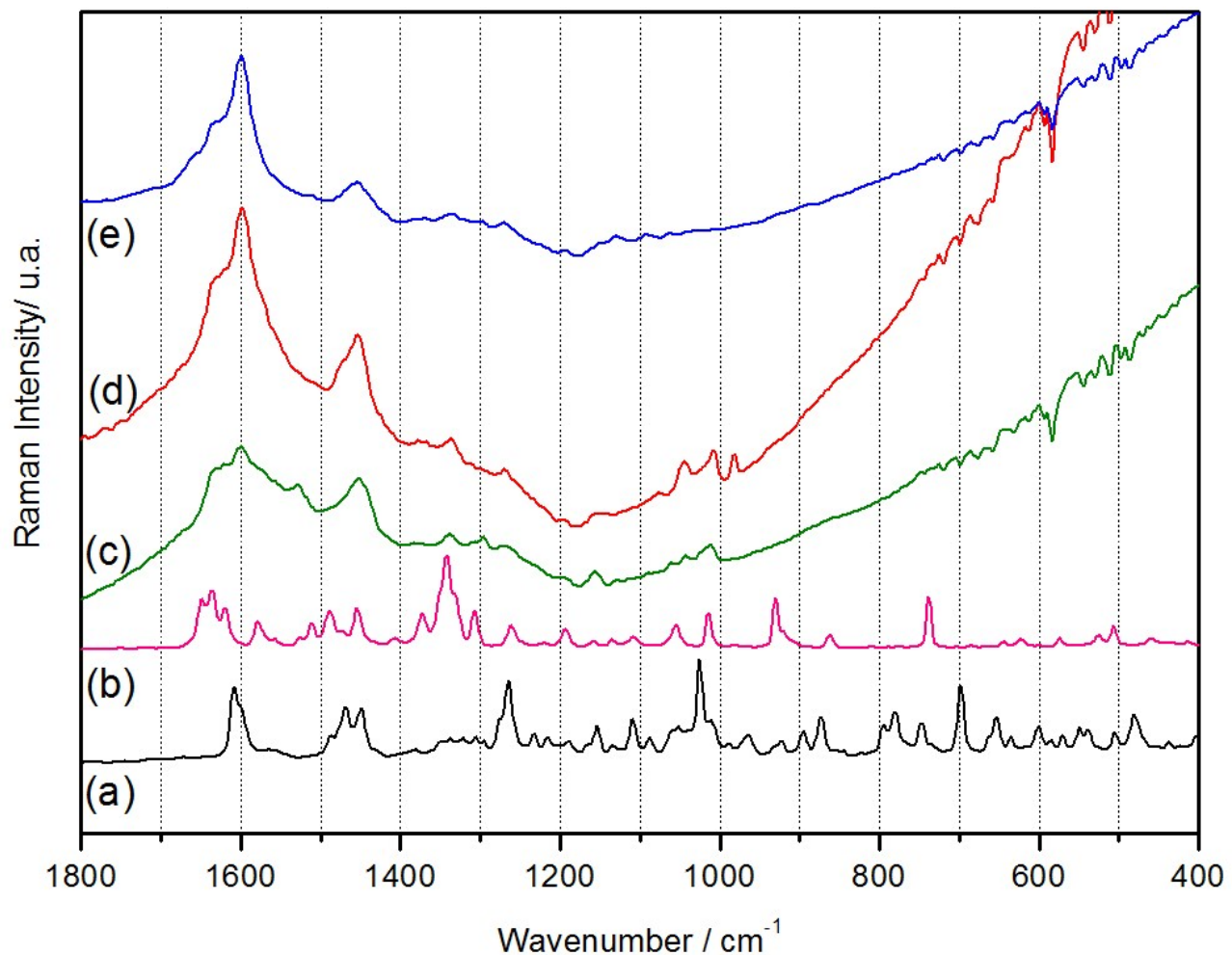


Figure S12. JB sample: (a) PR; (b) FP; (c) crude extract; (d) infusion and (e) bark.

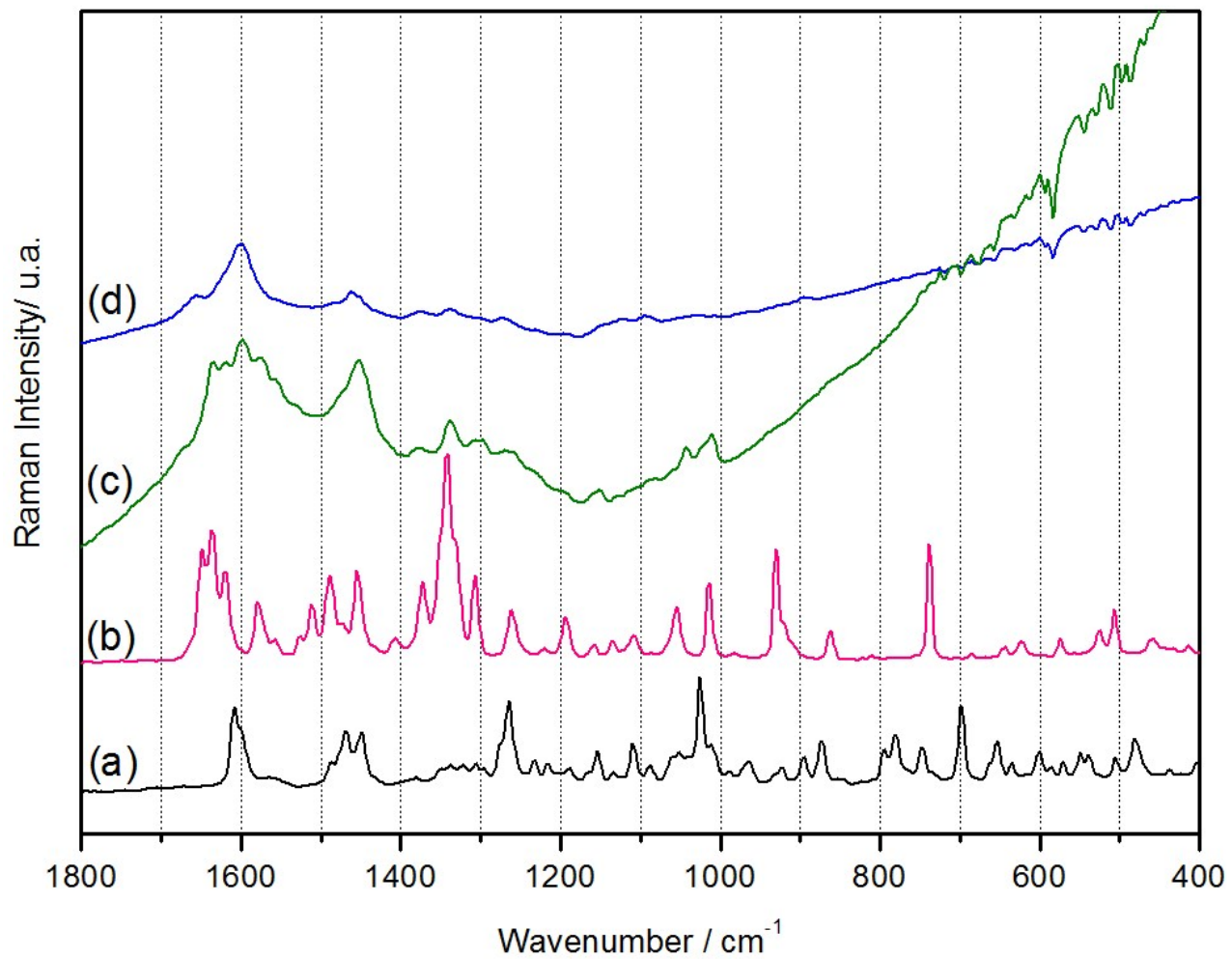


Figure S13. MAT06 sample: (a) PR; (b) FP; (c) crude extract and (d) bark.

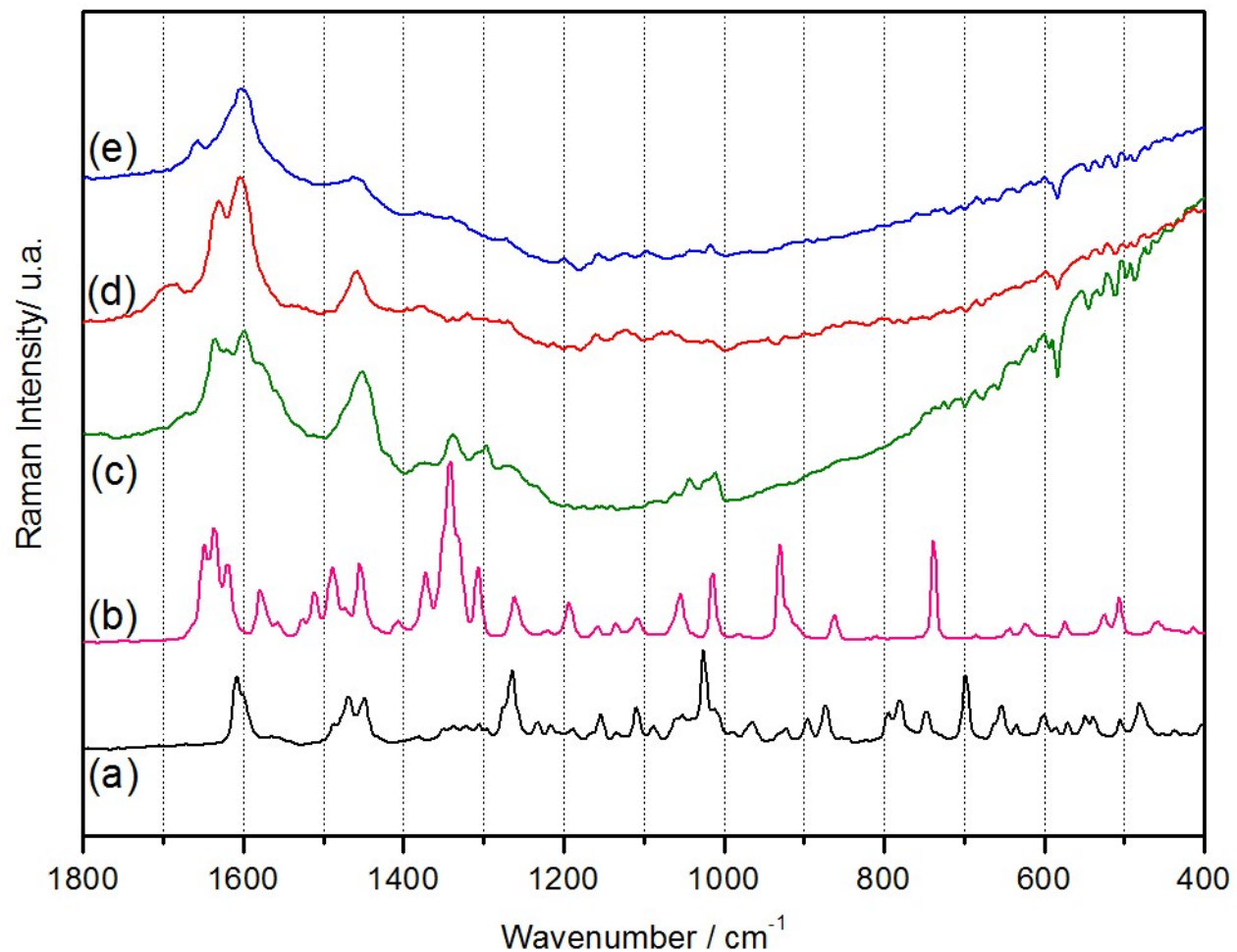


Figure S14. MAT09 sample: (a) PR; (b) FP; (c) crude extract; (d) infusion and (e) bark.

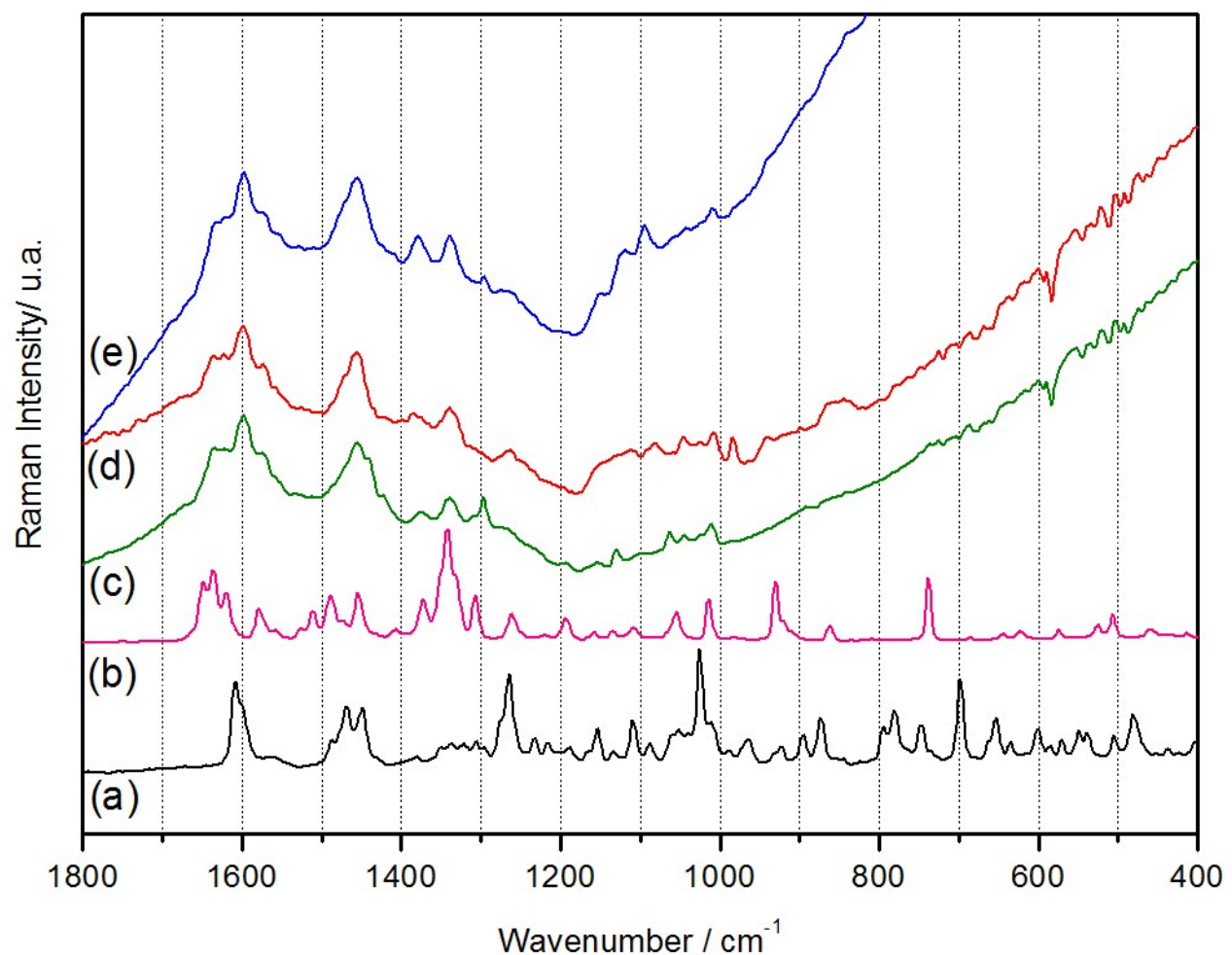


Figure S15. PV sample: (a) PR; (b) FP; (c) crude extract; (d) infusion and (e) bark.

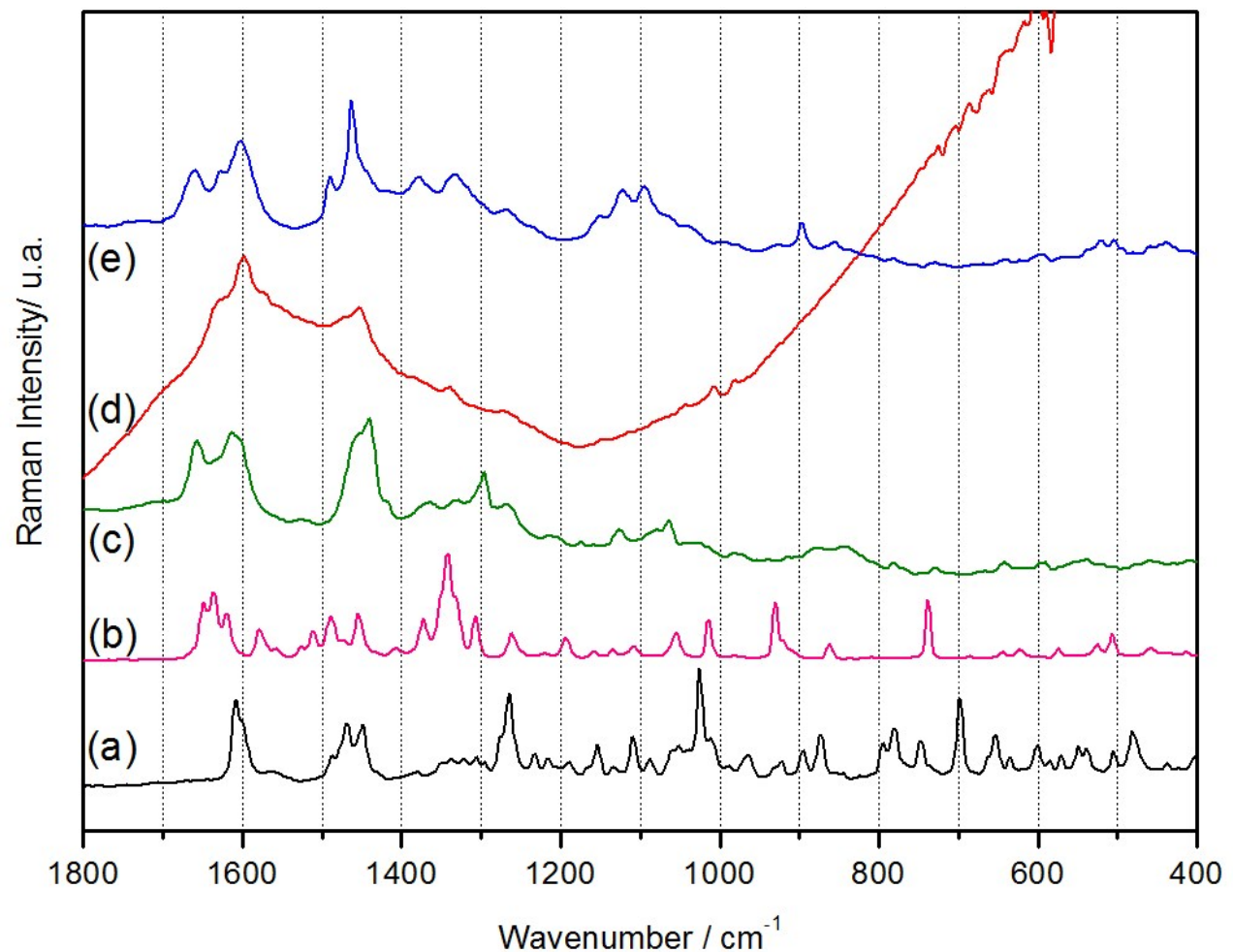


Figure S16. PM sample: (a) PR; (b) FP; (c) crude extract; (d) infusion and (e) bark.

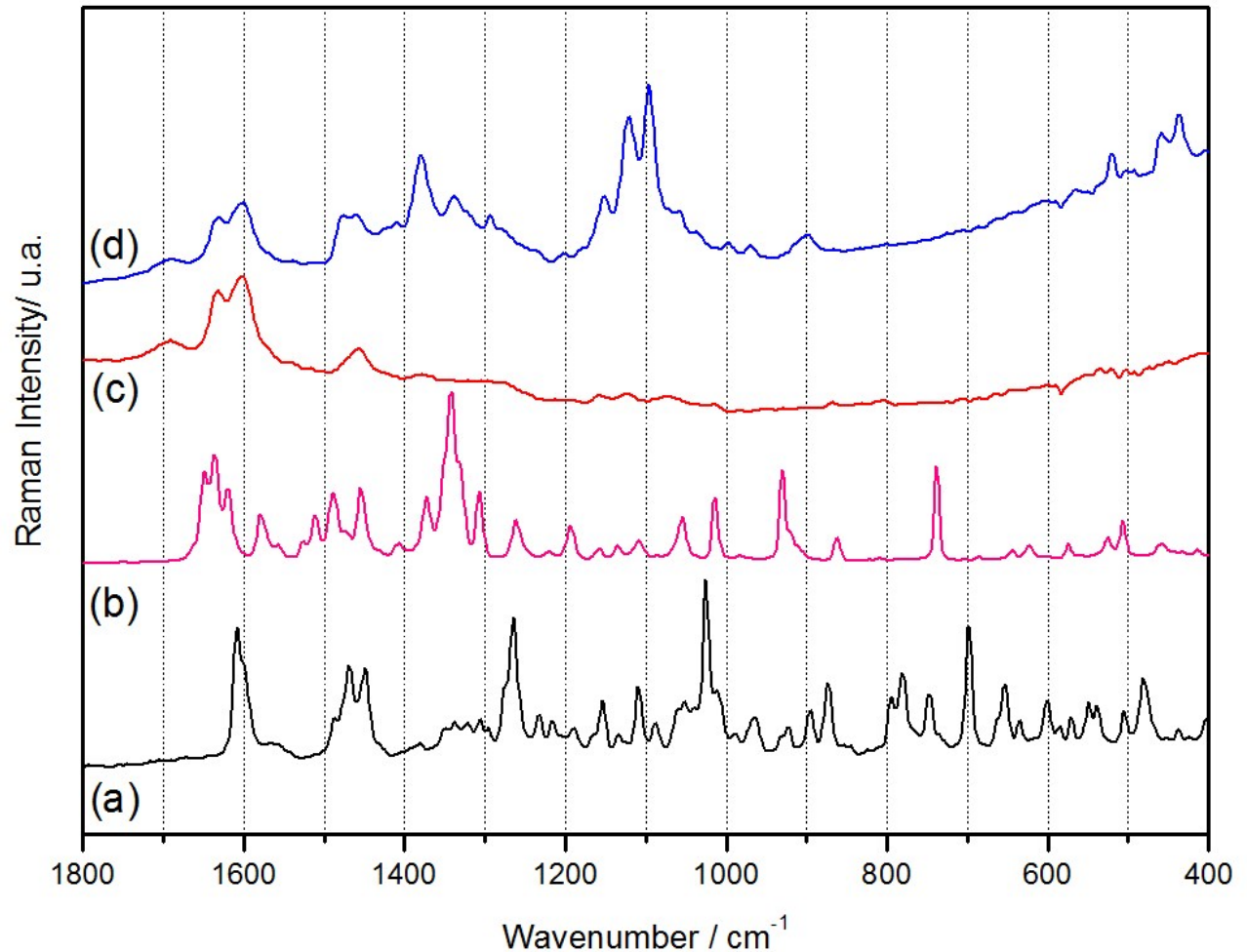


Figure S17. P4 sample: (a) PR; (b) FP; (c) infusion and (d) bark.

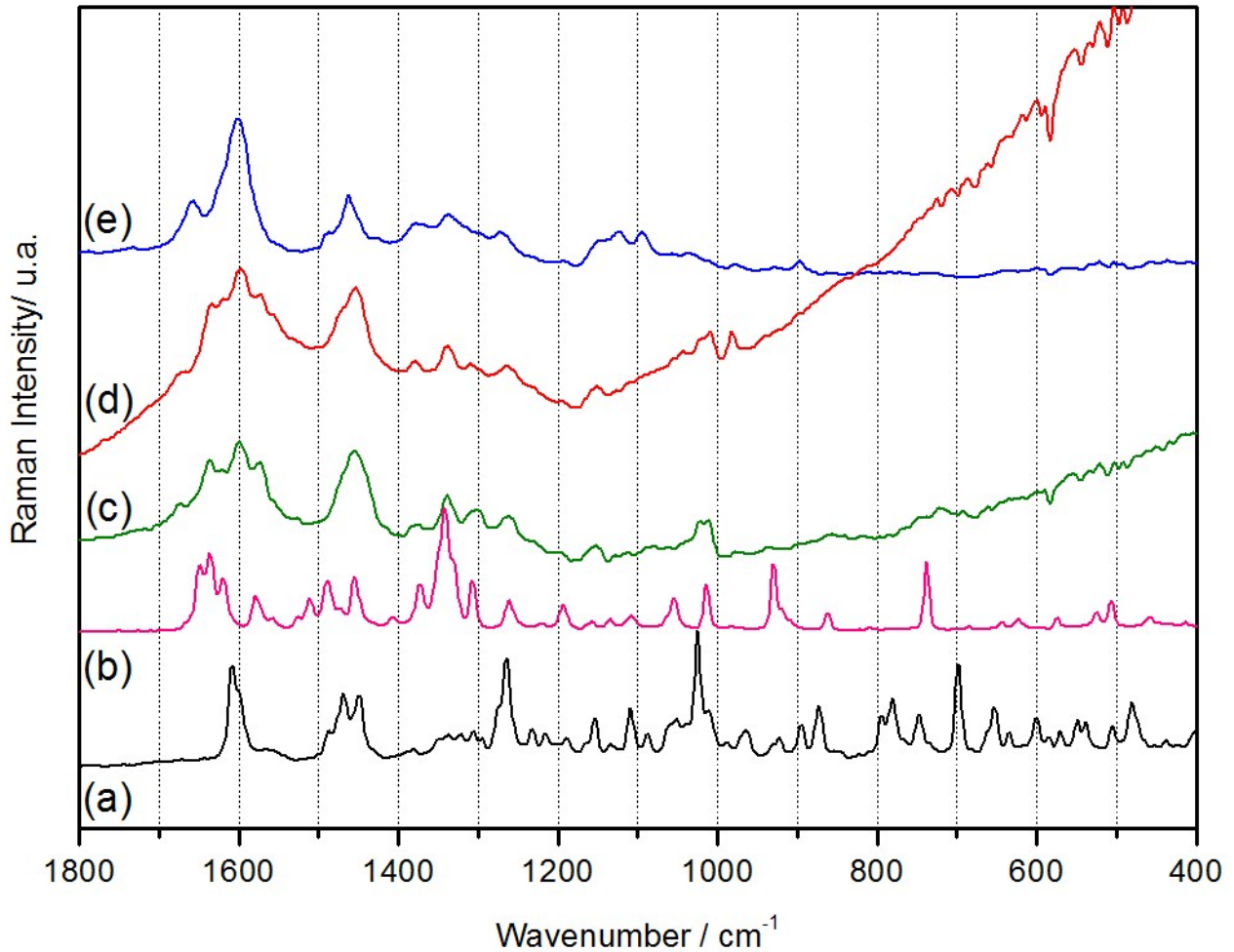


Figure S18. SMAR sample: (a) PR; (b) FP; (c) crude extract; (d) infusion and (e) bark.

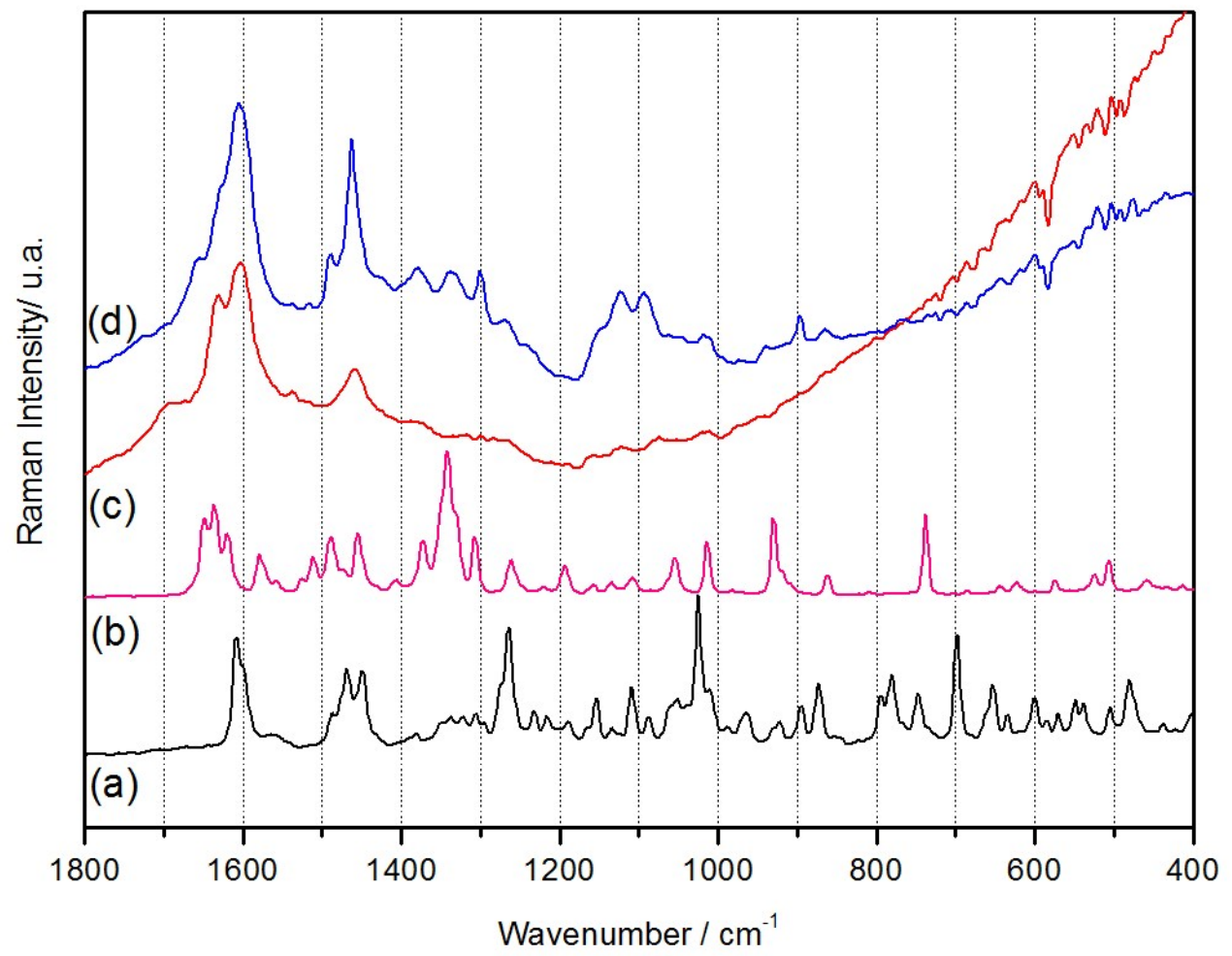


Figure S19. AN sample: (a) PR; (b) FP; (c) infusion and (d) bark.

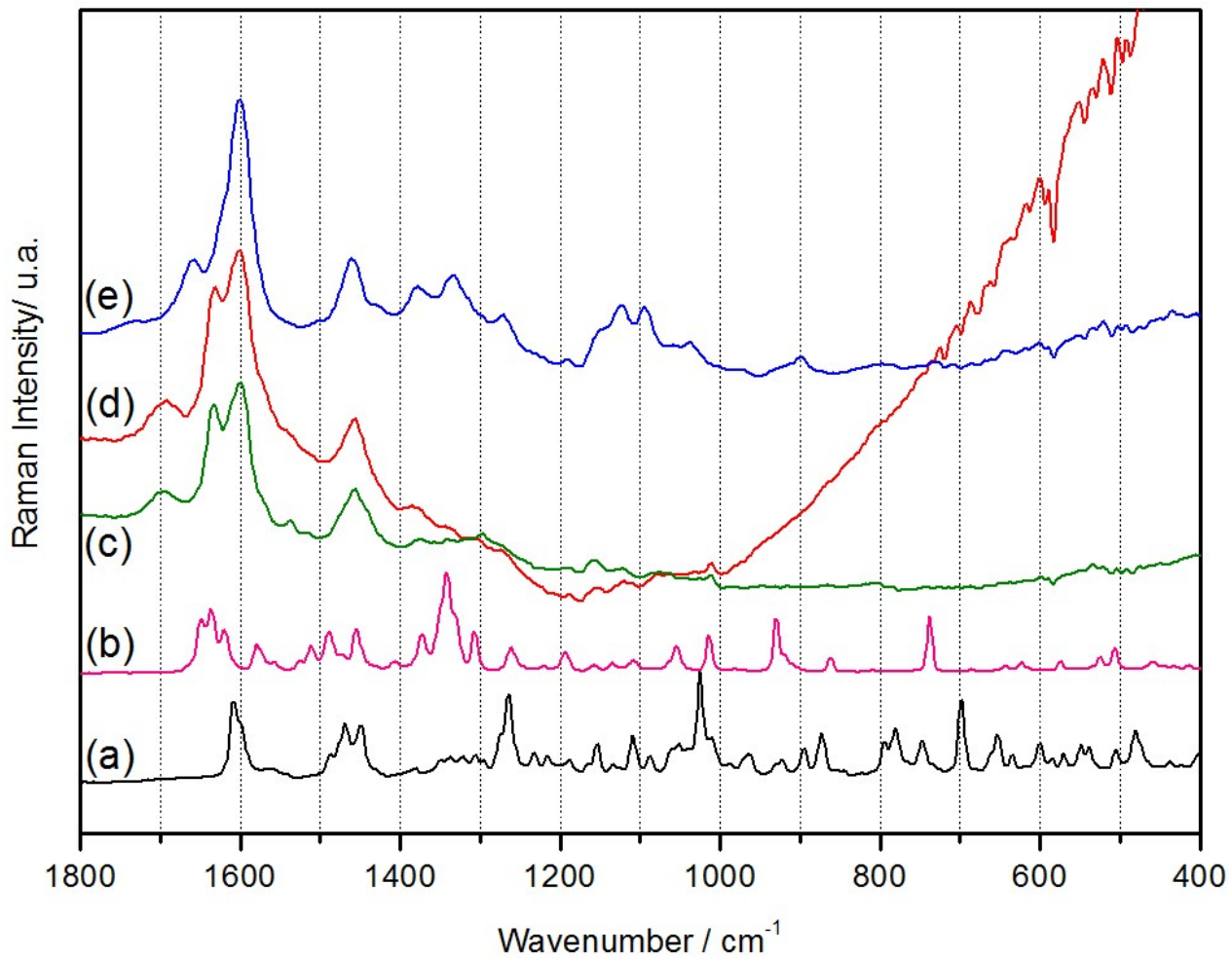


Figure S20. CHACIA sample: (a) PR; (b) FP; (c) crude extract; (d) infusion and (e) bark.

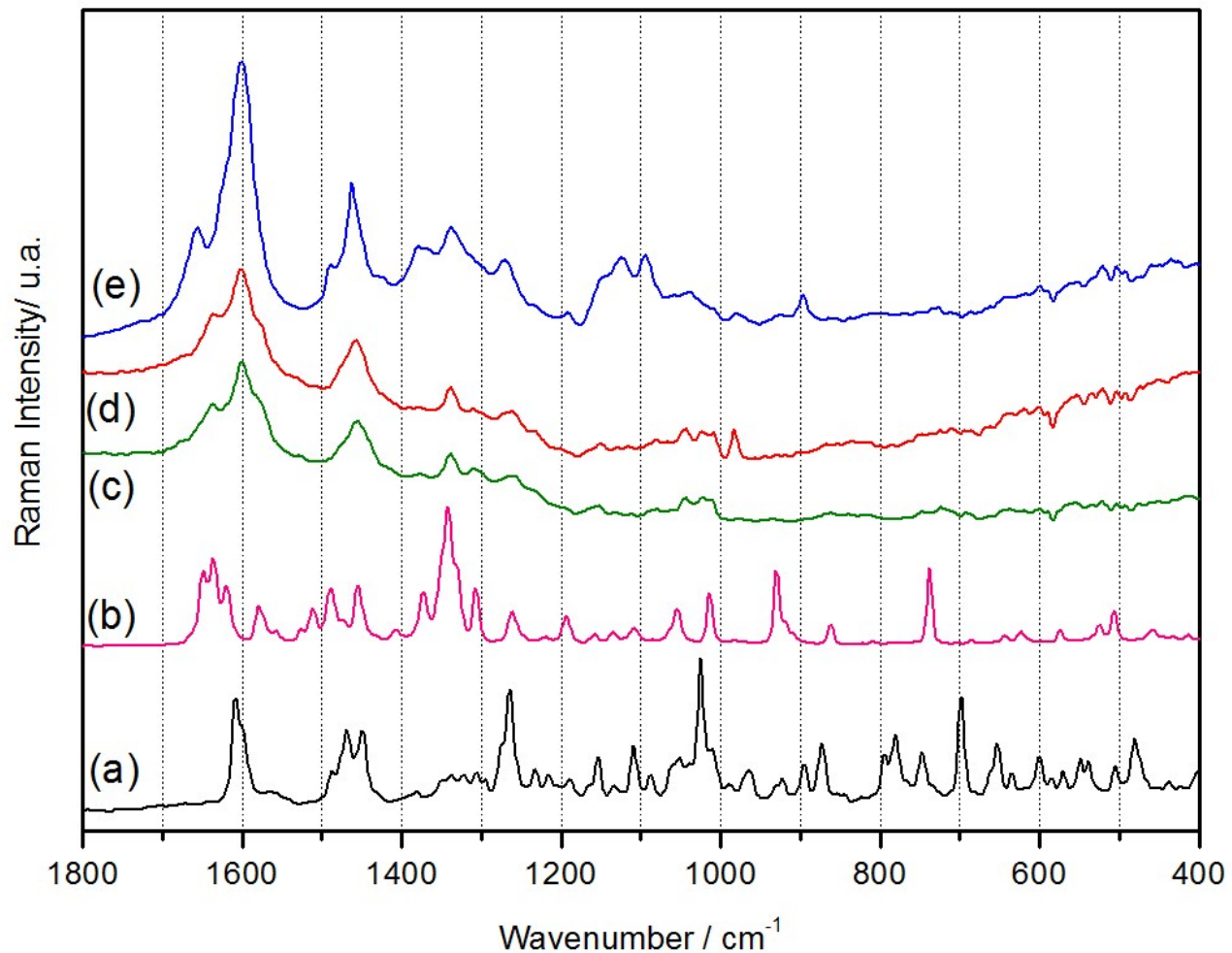


Figure S21. FEILC sample: (a) PR; (b) FP; (c) crude extract; (d) infusion and (e) bark.

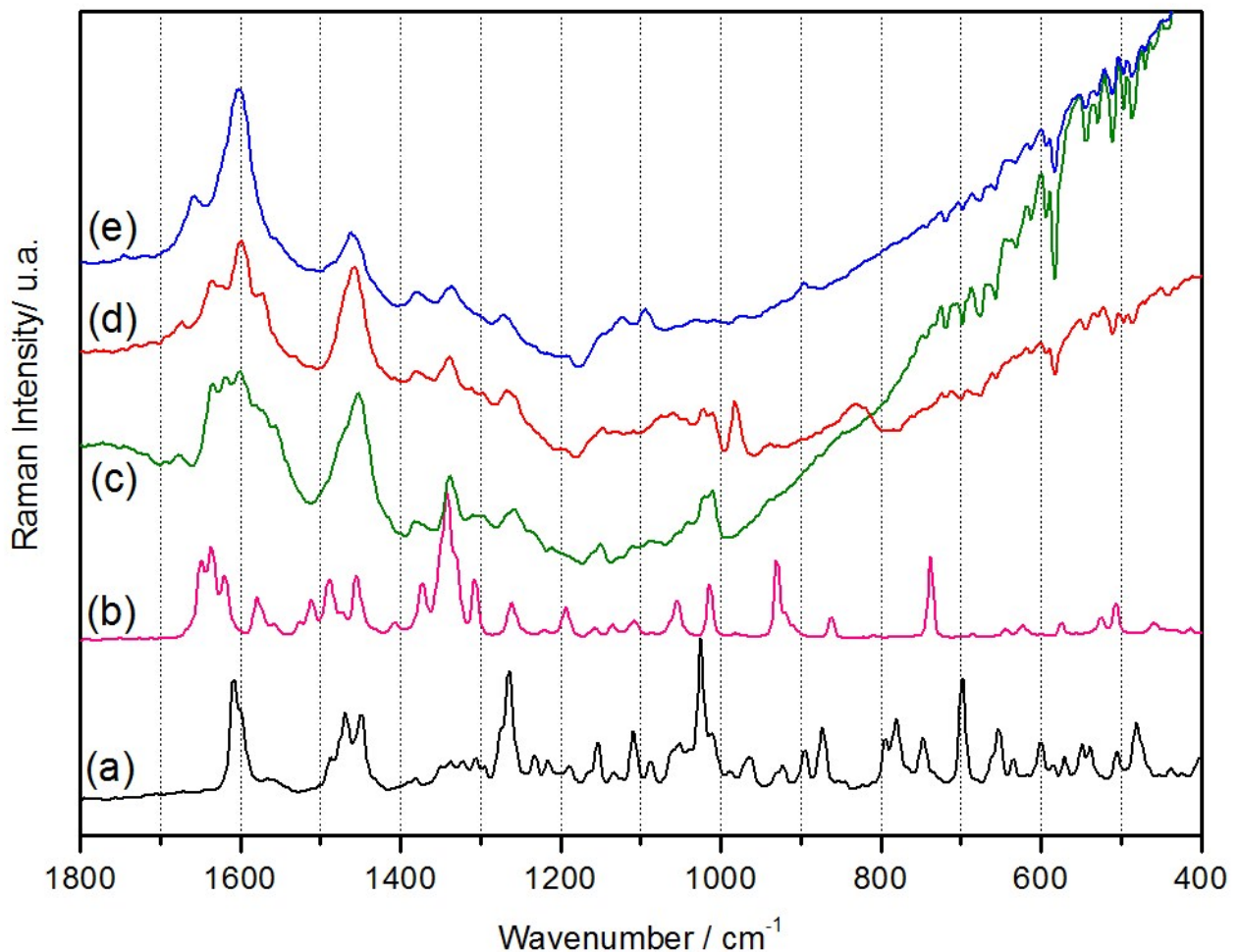


Figure S22. FEILSF sample: (a) PR; (b) FP; (c) crude extract; (d) infusion and (e) bark.

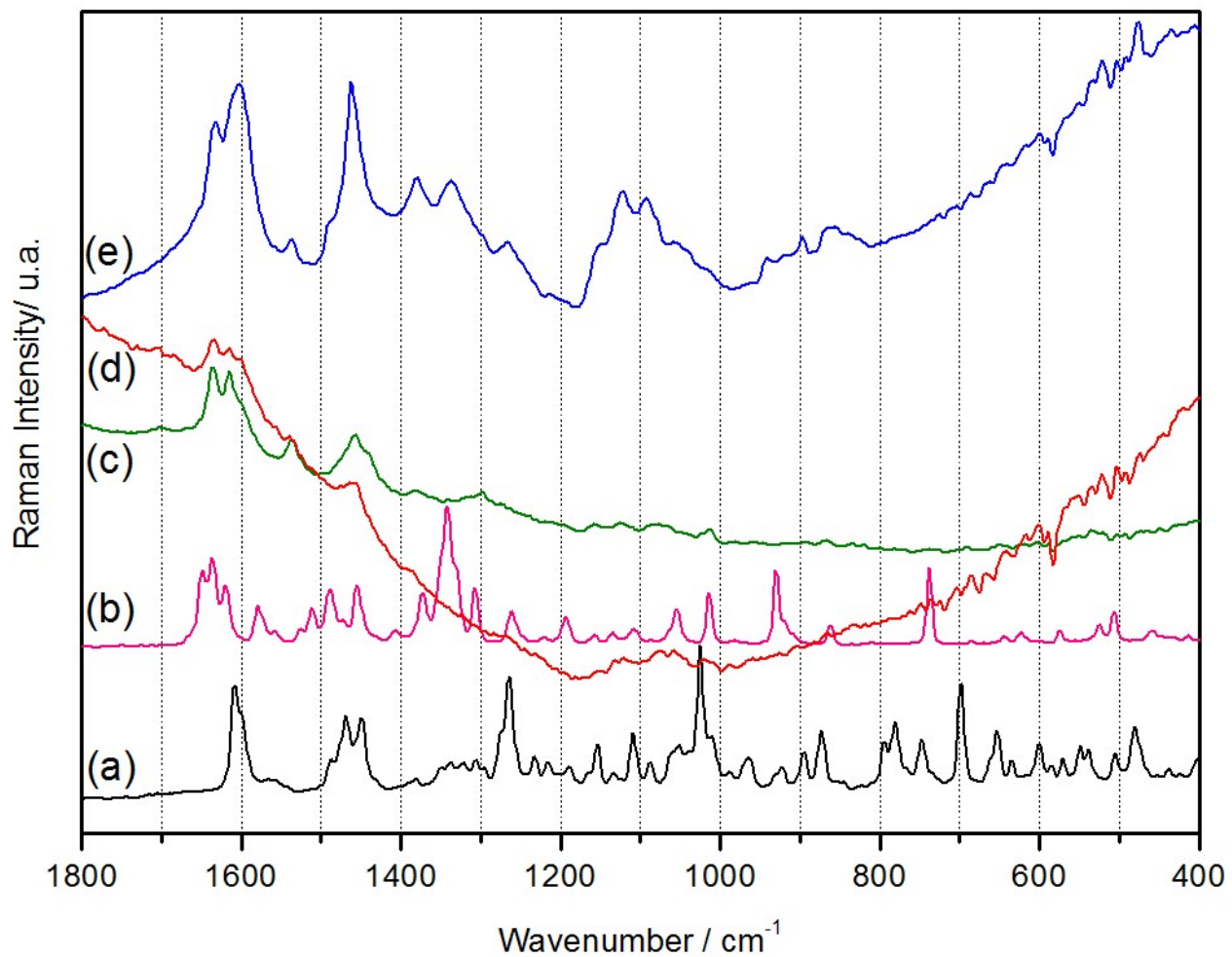


Figure S23. JUV sample: (a) PR; (b) FP; (c) crude extract; (d) infusion and (e) bark.

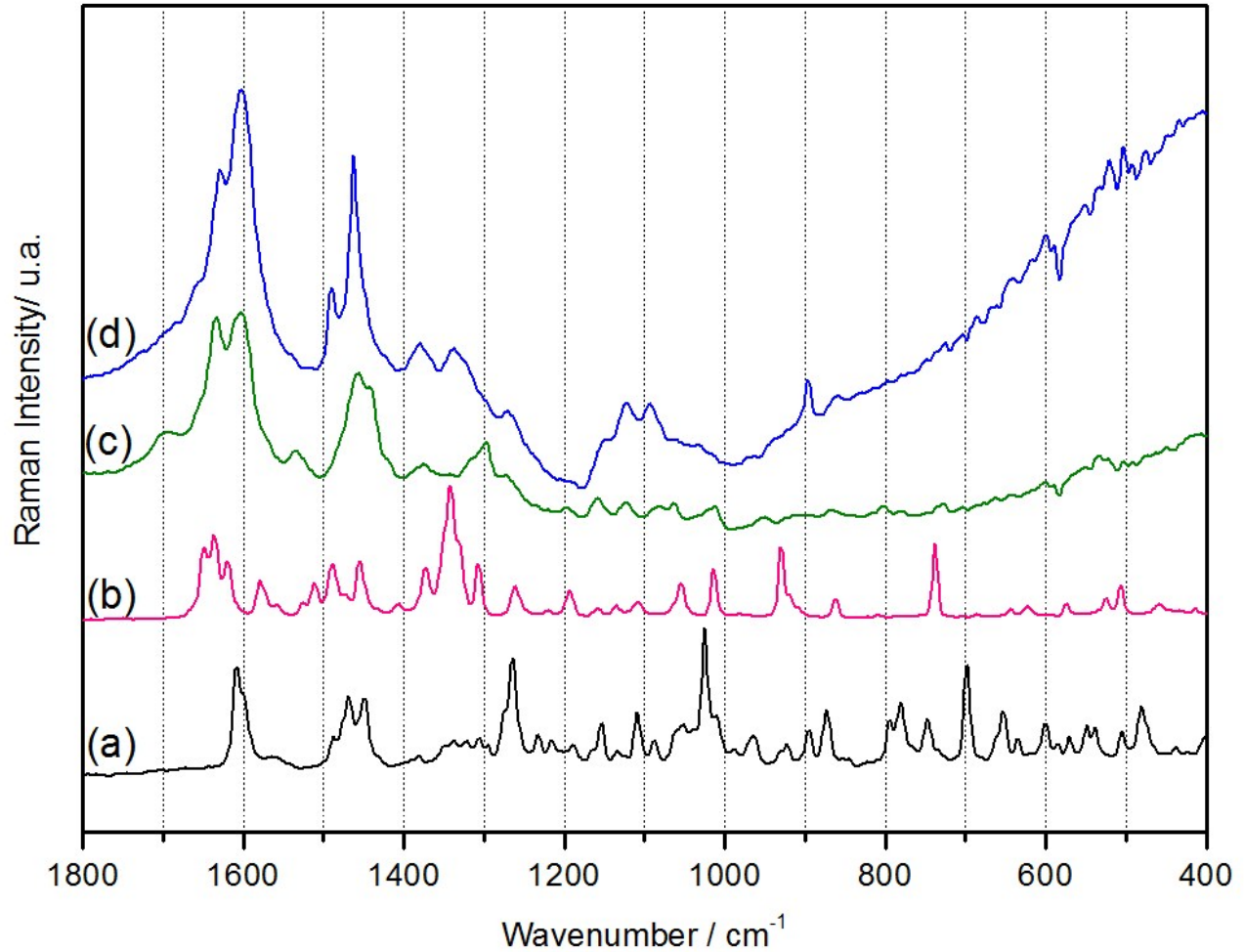


Figure S24. SA sample: (a) PR; (b) FP; (c) crude extract and (d) bark.

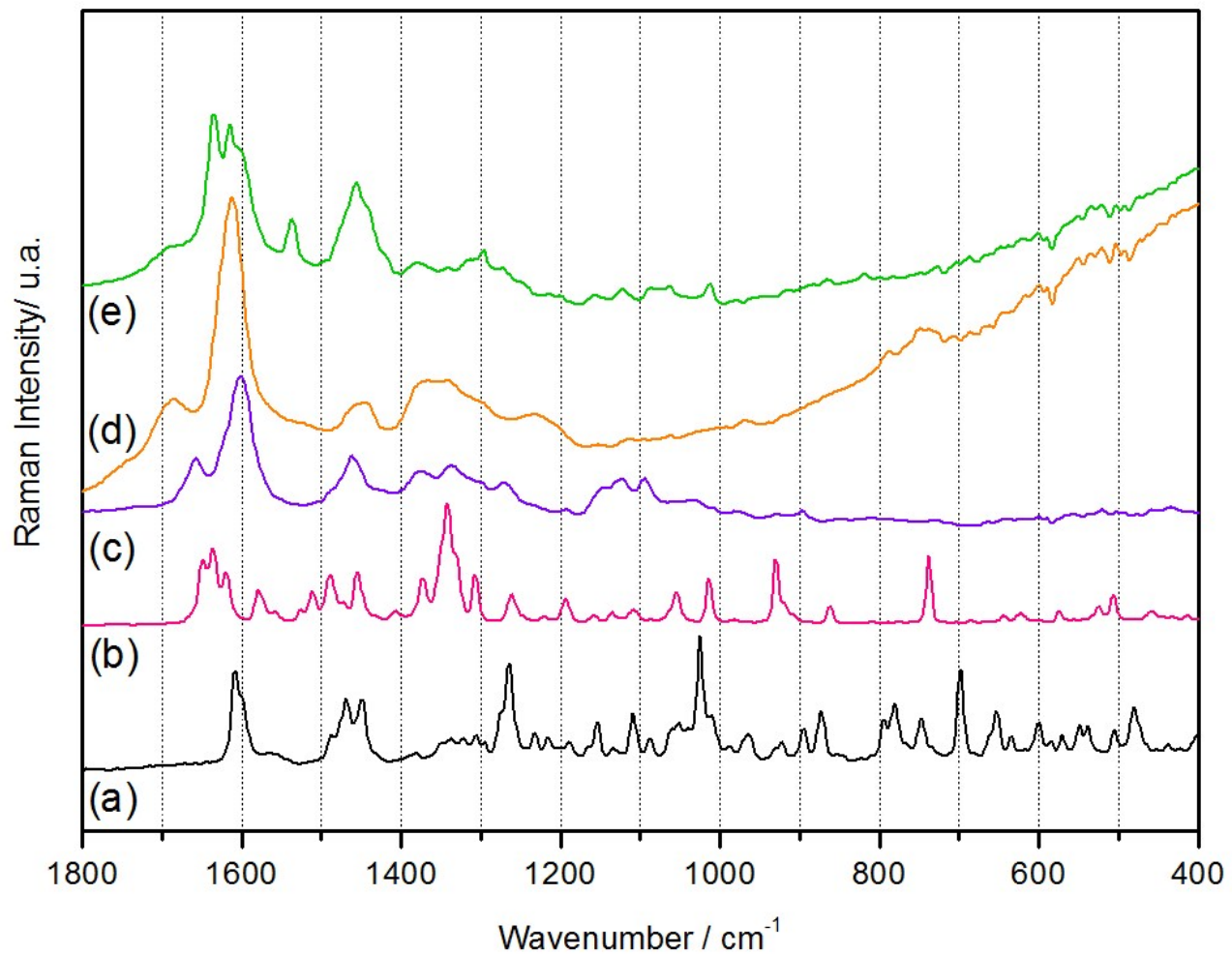


Figure S25. TING; UM and LM samples: (a) PR; (b) FP; (c) TING; (d) UM and (e) LM.

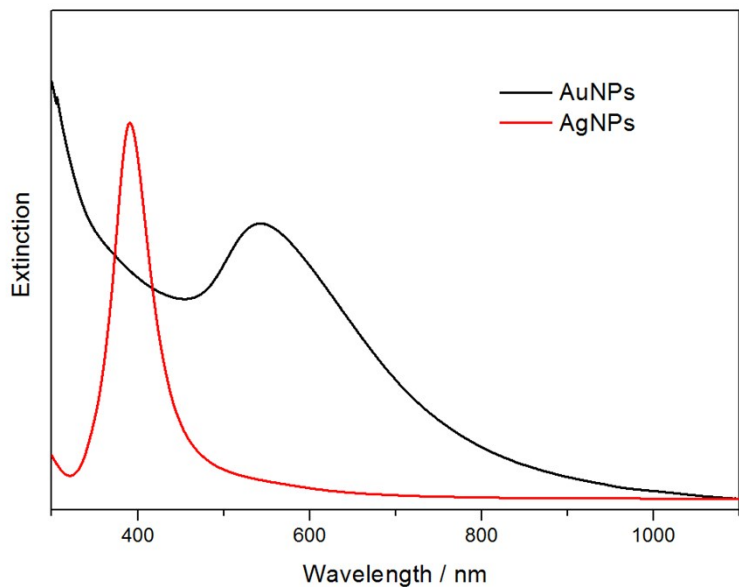


Figure S26. UV-VIS spectra of AgNPs and AuNPs in aqueous suspension.

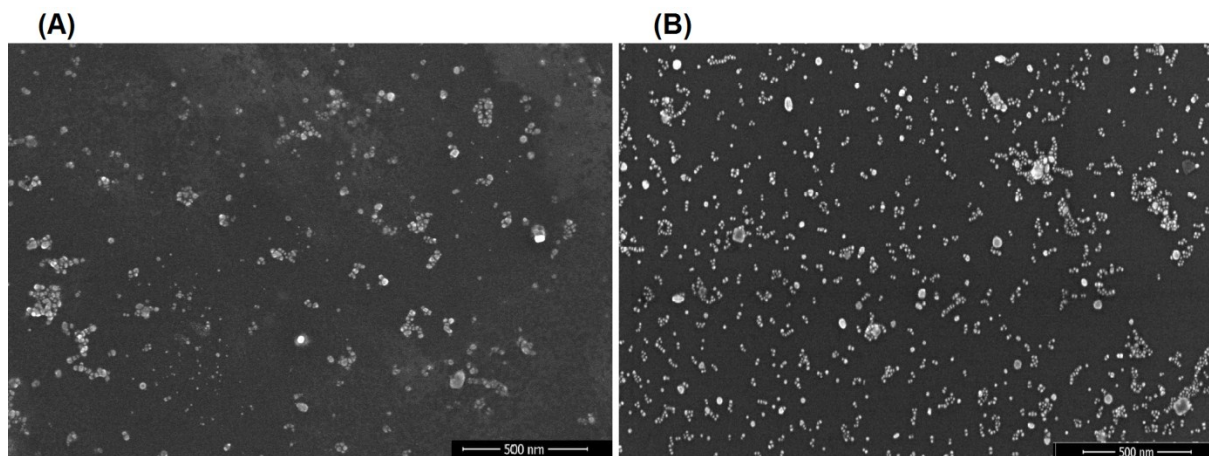


Figure 27. Scanning Electron Microscopy (SEM) images of AgNPs (a) and AuNPs (B). Aqueous suspensions dried on silicon plate.

The SEM images shows the drying process led to the formation of clusters, for both metals, which are in resonance with 1064 nm wavelength laser line that was used in SERS experiments.

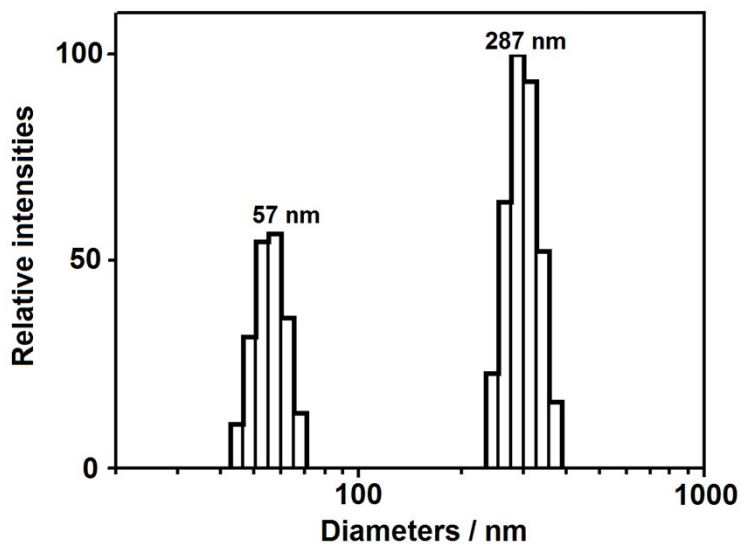


Figure S28. Dynamic Light Scattering (DLS) of AuNPs suspension.

The DLS Of AuNPs suspension showed the presence of two size distribution. The first has a maximum at 57 nm indicating the average size of isolated nanoparticles and the latter presents a maximum at 287 nm related with clusters formed in the aqueous medium.

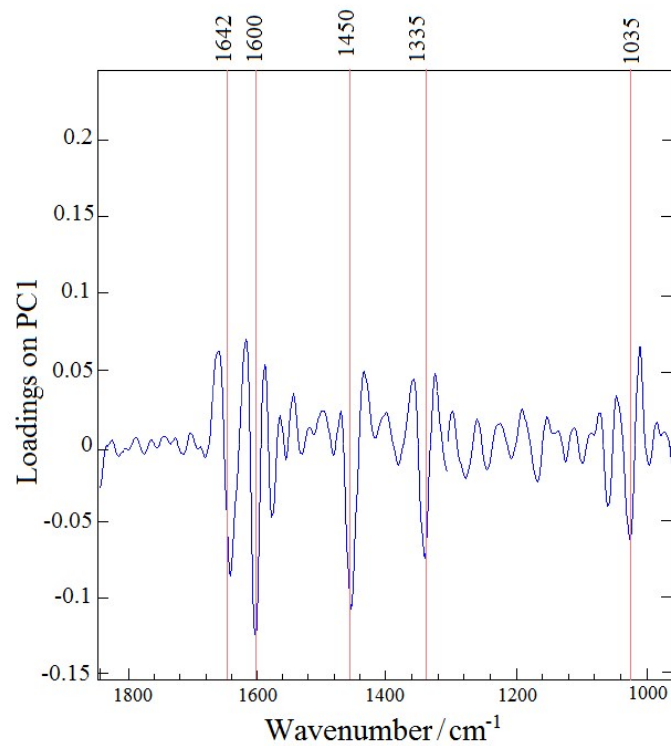


Figure S29. Graph of the loadings of PC1 versus Raman wavenumbers for the PCA model.

Table S1. Collecting sites and sample types used for Raman and PCA analyses.

Sample number (PCA) and processing type**			Code	Source
Bark	INF	EE		
1	2	3	AC	Market
4	5	6	ACVL	Market
7	8	9	EN	Market
	10	11	FJ	Market
12	13	14	JB	Collection (reference)
15		16	MAT06	Collection
17	18	19	MAT09	Collection
20	21	22	MM	Market
23	24	25	PV	Phytotherapeutic 1
26	27	28	PM	Collection
29			P4	Phytotherapeutic 2
	30	31	SMAR	Market
		32	FEILM	Market
33	34		AN	Market
35	36	37	CHACIA	Market
38	39	40	FEILC	Market
41	42	43	FEILSF	Market
44	45	46	JUV	Market
47		48	SA	Market
49			TING	Collection (reference)
		50	UM	Market
		51	LM	Market
52			FP	Experimental Section
53			PR	

** INF: infusion; EE: ethanol crude extract.

Tables

Table S2. Comparison between experimental and theoretical Raman spectra of PR and GC, respectively.

Exp.	B3LYP	BHandH	BHandHLYP	PBE1PBE	Tentative assignment
1608 s	1637	1741	1716	1667	$\nu(\text{C}=\text{C})_{\text{A}}$
1602 sh	1626	1724	1700	1653	$\nu(\text{C}=\text{C})_{\text{A}}$
1488 sh	1514	1555	1575	1523	$\delta(\text{CH}_2)_{\text{D}} + \nu(\text{C-C,C-N})_{\text{A,B}}$
1470 m	1505	1539	1563	1498	$\nu(\text{C-C,C-N})_{\text{A,B}} + \delta(\text{CH}_2)_{\text{E}}$
1449 m	1486	1522	1544	1485	$\delta(\text{CH}_2,\text{CH}_3)_{\text{sd}}$
1430 w	-	1494	1535	1472	$\nu(\text{C-C,C-N})_{\text{A,B}} + \delta(\text{NH})_{\text{B}}$
1337 w	1356	1419	1445	1381	$\nu(\text{C-C})_{\text{A,B}} + \delta(\text{CC})_{\text{C}}$
1321 vw	1349	1390	1432	1352	$\nu(\text{C-C})_{\text{A,B}} + \delta(\text{CH},\text{CH}_2)$
1306 w	1334	1371	1415	1333	$\nu(\text{C-C,C-N})_{\text{B,C,D,E}}$
1275 sh	1276	1330	1392	1301	$\delta(\text{CH})_{\text{B,C,D,sd}}$
1264 s	1267	1319	1311	1284	$\nu(\text{C-C,C-N})_{\text{A,B}}$
1155 w	1171	1225	1209	1187	$\delta(\text{CH})_{\text{A,C,D,sd}} + \delta(\text{CC})_{\text{A,B,C,D,E,sd}}$
1109 w	1109	1187	1160	1128	$\delta(\text{CH})_{\text{A,C,D,sd}} + \delta(\text{CC})_{\text{A,B,C,D,E,sd}}$
1025 s	1041	1079	1075	1047	$\nu(\text{C-C})_{\text{A,Br}}$
1012 w	1030	1056	1049	1019	$\nu(\text{C-C,C-O})_{\text{sd}} + \nu(\text{C-C})_{\text{C,D,E}}$
795 m	808	817	815	893	$\delta(\text{CH}_2)$
780m	785	788	793	879	$\delta(\text{CC})_{\text{A,B,C,D,E}}$
748 m	756	769	758	788	$\delta(\text{CC})_{\text{A,oop}}$
700 m	714	745	744	719	$\nu(\text{C-C})_{\text{B,C,D,Br}}$
653 w	655	677	678	659	$\delta(\text{CC})_{\text{A,B}}$

s: strong; m: media; w: weak; l: large; vw: very weak; vs: very strong, sh: shoulder.

Table S3. Comparison between experimental and theoretical and Raman spectra of FP.

Exp.	B3LYP	BHandH	BHandHLYP	PBE1PBE	Tentative assignment
1648 s	1672	1788	1766	1711	$\nu(C=C, C-N)_D$
1637 s	1643	1751	1722	1677	
1620 s	1609	-	1683	-	$\nu(C=C, C-N)_{A,B}$
1579 m	1593	1705	1617	1578	$\nu(C=C)_{A,B,C}$
1511 m	1552	1637	1575	1539	$\nu(C=C)_{A,B,C}$
1488 m	1499	1562	1555	1513	$\nu(C=N)_B + \nu(C=C)_C$
1473	1465	-	-	-	$\delta(CH_2, CH_3) + \delta(CH)_D$
1456 m	1444	1501	1491	1450	$\delta(CH_2, CH_3)$
1407 w	1431	-	-	-	$\nu(C-N)_{B,C} + \nu(C-C)_D$
1373 m	1360	1448	1419	1392	$\nu(C-C, C-N)_{A,B,C,D}$
1342 vs [#]	1342	1423	1397	1377	$\nu(C-C, C-N)_{A,B,C,D} + \nu(C_D-C_{sd})$
1330 sh	1308	1405	-	1348	$\nu(C-C, C-N)_{A,B,C,D} + \nu(C_D-C_{sd})$
1308 m	1298	1387	1358	1319	$\nu(C-C, C-N)_{A,B,C,D} + \nu(C_D-C_{sd})$
1262 m	1262	1362	1337	1282	$\nu(C-N)_{B,C} + \nu(C-C)_D$
1192 m	1206	1318	1294	1222	$\nu(C_D-C_{sd})$
1055	1071	1115	1152	1115	$\nu(C-C, C-N)_{A,B,C,D}$
1015 m	1016	1057	1114	1080	$\nu(C-C)_{A,Br}$
930 m	922	1059	1055	1032	$\nu(C-C)_{sd} + \nu(C_D-C_{sd}) + \delta(C-C)_{C,D}$
860 w	857	895	890	867	$\delta(C-C, C-N)_{A,B,C,D,oop}$ $\nu(C-N)_{C,D,E}$
738 s	734	773	762	744	$\nu(C-C, C-N)_{A,B,C,D,Br}$

s: strong; m: media; w: weak; l: large; vw: very weak; vs: very strong, sh: shoulder.

Table S4. Lowest deviation for C-N_{indole} and C-C_{ring} bonds calculated for GC and FP.

Functional	GC		FP	
	C-N _{indole}	C-C _{ring}	C-C _{indole}	C-C _{ring}
B3LYP	1.393	1.399	1.339	1.383
PBE1PBE	1.386	1.390	1.334	1.379
BHandH	1.372	1.375	1.320	1.364
BHandHLYP	1.385	1.382	1.328	1.369
Literature*	1.391	1.363	1.391	1.363

*Wulf, G. D. (2012). Estruturas Cristalinas e Moleculares de indóis 1,3-Substituidos . (Master's thesis, Universidade Federal de São Carlos, São Carlos, Brazil). Retrieved from <https://repositorio.ufscar.br/bitstream/handle/ufscar/6542/4692>.

Table S5. Comparison between experimental and theoretical Raman spectra, including Raman shifts and relative errors of PR and GC, respectively, for different base sets.

Exp	B3LYP	σ	E_r	BHandH	σ	E_r	BHandHLYP	σ	E_r	PBE1PBE	σ	E_r
1608	1637	29	1.8	1741	133	8.3	1716	108	6.7	1667	59	3.7
1602	1626	24	1.5	1724	122	7.6	1700	98	6.1	1653	51	3.2
1488	1514	26	1.7	1555	67	4.5	1575	87	5.8	1523	35	2.4
1470	1505	35	2.4	1539	69	4.7	1563	93	6.3	1498	28	1.9
1449	1486	37	2.6	1522	73	5.0	1544	95	6.6	1485	36	2.5
1430	-	-	-	1494	64	4.5	1535	105	7.3	1472	42	2.9
1337	1356	19	1.4	1419	82	6.1	1445	108	8.1	1381	44	3.3
1321	1349	28	2.1	1390	69	5.2	1432	111	8.4	1352	31	2.3
1306	1334	28	2.1	1371	65	5.0	1415	109	8.3	1333	27	2.1
1275	1276	1	0.1	1330	55	4.3	1392	117	9.2	1301	26	2.0
1264	1267	3	0.2	1319	55	4.4	1311	47	3.7	1284	20	1.6
1155	1171	16	1.4	1225	70	6.1	1209	54	4.7	1187	32	2.8
1109	1109	0	0.0	1187	78	7.0	1160	51	4.6	1128	19	1.7
1025	1041	16	1.6	1079	54	5.3	1075	50	4.9	1047	22	2.1
1012	1030	18	1.8	1056	44	4.3	1049	37	3.7	1019	7	0.7
795	808	13	1.6	817	22	2.8	815	20	2.5	893	98	12.3
780	785	5	0.6	788	8	1.0	793	13	1.7	879	99	12.7
748	756	8	1.1	769	21	2.8	758	10	1.3	788	40	5.3
700	714	14	2.0	745	45	6.4	744	44	6.3	719	19	2.7
653	655	2	0.3	677	24	3.7	678	25	3.8	659	6	0.9

Table S6. Comparison between experimental and theoretical Raman spectra, including Raman shifts and relative errors of FP, for different base sets.

Exp	B3LYP	σ	E_r	BHandH	σ	E_r	BHandHLYP	σ	E_r	PBE1PBE	σ	E_r
1648	1672	24	1.5	1788	140	8.5	1766	118	7.2	1711	63	3.8
1637	1643	6	0.4	1751	114	7.0	1722	85	5.2	1677	40	2.4
1620	1609	11	0.7	-	-	-	1683	63	3.9	-	-	-
1579	1593	14	0.9	1705	126	8.0	1617	38	2.4	1578	1	0.1
1511	1552	41	2.7	1637	126	8.3	1575	64	4.2	1539	28	1.9
1488	1499	11	0.7	1562	74	5.0	1555	67	4.5	1513	25	1.7
1473	1465	8	0.5	-	-	-	-	-	-	-	-	-
1456	1444	12	0.8	1501	45	3.1	1491	35	2.4	1450	6	0.4
1407	1431	24	1.7	-	-	-	-	-	-	-	-	-
1373	1360	13	0.9	1448	75	5.5	1419	46	3.4	1392	19	1.4
1342	1342	0	0.0	1423	81	6.0	1397	55	4.1	1377	35	2.6
1330	1308	22	1.7	1405	75	5.6	-			1348	18	1.4
1308	1298	10	0.8	1387	79	6.0	1358	50	3.8	1319	11	0.8
1262	1262	0	0.0	1362	100	7.9	1337	75	5.9	1282	20	1.6
1192	1206	14	1.2	1318	126	10.6	1294	102	8.6	1222	30	2.5
1055	1071	16	1.5	1115	60	5.7	1152	97	9.2	1115	60	5.7
1015	1016	1	0.1	1057	42	4.1	1114	99	9.8	1080	65	6.4
930	922	8	0.9	1059	129	13.9	1055	125	13.4	1032	102	11.0
860	857	3	0.3	895	35	4.1	890	30	3.5	867	7	0.8
738	734	4	0.5	773	35	4.7	762	24	3.3	744	6	0.8

Table S7. GC B3LYP cartesian coordinates.

C	-4.67552	0.41494	-0.00918
C	-3.74825	0.90377	-0.93644
C	-2.44622	0.41004	-0.88765
C	-2.06970	-0.55786	0.05889
C	-3.00073	-1.03838	0.96612
C	-4.31348	-0.54399	0.93679
H	-5.69314	0.79273	-0.02908
H	-4.03997	1.64673	-1.67235
H	-2.72497	-1.79245	1.69775
H	-5.04585	-0.90898	1.64864
N	-1.36549	0.71000	-1.71429
H	-1.36141	1.59285	-2.20293
C	-0.11973	0.26997	-1.05873
C	0.66283	1.40502	-0.30077
C	-0.62315	-0.94177	-0.18809
H	0.55260	-0.10183	-1.83417
C	1.56213	0.86768	0.84968
H	1.30994	1.88648	-1.04521
C	0.25564	-1.22072	1.06486
C	0.72296	0.01758	1.80663
H	-0.33281	-1.85434	1.74175
C	-0.23031	2.54194	0.22449
H	-0.88601	2.91072	-0.57322
H	-0.87340	2.20630	1.04781
O	0.62754	3.60150	0.66004
H	0.08474	4.31544	1.00799
C	-0.48567	-2.29837	-0.96221
H	-1.40854	-2.87933	-0.89159
H	-0.29786	-2.12762	-2.02586
C	0.69598	-3.04396	-0.25646
N	1.37257	-2.05568	0.59392
C	2.41696	-1.33405	-0.15905
C	2.80146	0.02683	0.44527
C	3.78732	0.79228	-0.45608
H	3.36042	0.91225	-1.46071
H	3.90234	1.80659	-0.05265
C	5.17450	0.14619	-0.57593
H	5.84719	0.77653	-1.16733
H	5.63135	0.00773	0.41126
H	5.13338	-0.83364	-1.06302

H	1.32044	-0.28094	2.67513
H	-0.14416	0.56505	2.18914
H	2.12705	-1.17900	-1.21370
H	3.29746	-1.98500	-0.18612
H	1.40166	-3.49533	-0.95923
H	0.30482	-3.84833	0.37724
H	3.32257	-0.17660	1.39290
H	1.94021	1.74882	1.37685

Table S8. FP B3LYP cartesian coordinates.

C	-2.94362	-1.41217	-0.28507
C	-1.58017	-1.47913	-0.22023
C	-3.59139	-0.14209	-0.27541
C	-0.78522	-0.31275	-0.14146
C	-2.81029	0.97252	-0.20399
C	-0.71137	2.10759	-0.06529
H	-1.31212	3.00545	-0.06728
C	0.66167	2.11490	0.00208
C	1.36710	0.91016	0.00028
C	0.62768	-0.33152	-0.07292
H	-3.22488	1.97245	-0.19880
H	1.16429	3.07500	0.05561
N	-1.42690	0.92398	-0.13550
C	-5.09675	-0.03165	-0.32920
H	-5.37929	1.00221	-0.55677
H	-5.46740	-0.64494	-1.16018
C	-5.78434	-0.47630	0.97441
H	-6.87217	-0.40009	0.87964
H	-5.54061	-1.51483	1.22110
H	-5.46992	0.14885	1.81658
H	-3.53692	-2.31816	-0.35096
H	-1.04012	-2.41804	-0.22927
C	3.88075	-1.67070	0.04316
C	2.68212	-0.93203	0.00810
C	2.73000	0.50690	0.05407
C	3.96280	1.17892	0.13371
C	5.12633	0.43104	0.16676
C	5.07954	-0.98452	0.12138
H	3.84903	-2.75458	0.00884
H	4.00589	2.26397	0.16872
H	6.08870	0.92873	0.22832
H	6.01213	-1.54040	0.14930
N	1.40326	-1.42408	-0.06838